https://doi.org/10.5194/egusphere-2026-3043
Preprint. Discussion started: 11 June 2026

A New Simple and Accurate Measure of Baroclinicity

Rhiannon Biddiscombe[1], Maarten Ambaum[1], and Ben Harvey[1, 2]

[1]Department of Meteorology, University of Reading, Reading, UK
[2]National Centre for Atmospheric Science, University of Reading, Reading, UK

Correspondence: Rhiannon Biddiscombe (R.Biddiscombe@PGR.Reading.ac.uk)

Abstract. Baroclinicity is the measure of baroclinic growth rate in the midlatitude storm tracks. Spatially, it defines the genesis region of the storm track and, temporally, it sets the activity of the storm track. Baroclinicity can be quantified with the Eady growth rate, which is proportional to the vertical shear of the zonal wind. This can alternatively be expressed as a meridional gradient of dry entropy via thermal wind balance. Both expressions of the Eady growth rate are equally valid given their derivation under the quasi-geostrophic approximations in which thermal wind balance is assumed. With a focus on the North Atlantic winter storm track, we demonstrate that variability in lower-tropospheric baroclinicity, averaged over a region encompassing the storm track, is determined almost entirely by lower-tropospheric dry entropy to the north of the storm track, with decreases in northward entropy corresponding to increases in baroclinicity. We use physical arguments as well as a linear regression to relate storm track baroclinicity to the mean dry entropy to the north of the storm track, demonstrating that variability in area mean baroclinicity of the storm track is mainly determined by processes on its poleward side, rather than by local-scale internal processes within the storm track itself. It also provides a much simplified physical picture to accurately describe the dynamics of the N. Atlantic storm track.

1 Introduction

The development of cyclones in the storm tracks is enabled by the presence of upstream regions of high baroclinicity (Blackmon et al., 1977; Simmons and Hoskins, 1979). Available potential energy (APE) in these pools of baroclinicity acts as fuel for the growth of eddies, eroding baroclinicity as the cyclones redistribute heat poleward and reducing the potential for the development of new systems (Blackmon et al., 1977; Ambaum and Novak, 2014). In the absence of eddies and high meridional heat flux, baroclinicity may be restored by diabatic processes until the storm track again becomes favourable to the development of baroclinic eddies (Ambaum and Novak, 2014).

The Eady model is a simplified quasi-geostrophic model which captures the key physics of baroclinic instability, and from it emerges the Eady growth rate which characterises the rate of growth of the fastest growing mode in the Eady model and is generally considered a good measure of observed eddy growth rate, even for more complex vertical profiles than in the original model setup (Eady, 1949; Lindzen and Farrell, 1980). While the Eady growth rate typically depends on vertical shear of the zonal wind, it can be rearranged to a number of equally valid expressions under the assumptions of quasi-geostrophy.

As the storm tracks are persistent features of the winter mid-latitude atmosphere, there must be mechanisms for the re-establishment of baroclinicity in the mid-latitudes (Hoskins and Valdes, 1990). The maintenance of the storm tracks relies on

https://doi.org/10.5194/egusphere-2026-3043
Preprint. Discussion started: 11 June 2026

the generation of APE, allowing for the development of weather systems. Many mechanisms exist for increasing APE in the atmosphere. APE can be generated over large areas by the advection of temperature anomalies, like during cold-air outbreaks, as stronger horizontal temperature gradients lead to steeper isentropic surfaces. Localised mesoscale events can also facilitate the generation of APE, with diabatic processes within the warm conveyor belt and dry intrusion of a cyclone generating APE favourable to the downstream development of cyclones (Federer et al., 2024).

Papritz and Spengler (2015) utilise a framework based on the slope of isentropic surfaces, where steeper slopes are indicative of higher APE, to analyse to evolution of barolinicity within the storm tracks. In this perspective, latent heating acts significantly to maintain baroclinicity in the storm tracks. While this framework characterises well local features and their contribution to the generation of baroclinic eddies, a physical understanding of baroclinicity and baroclinic instability depends on a larger-scale perspective in which the unstable mode of a baroclinic wave produces strong vorticity anomalies. While localised diabatic effects appear to facilitate cyclone intensification rates, cyclone clustering and other synoptic-scale features (Binder et al., 2016; Weijenborg and Spengler, 2020) it is not clear to what extent the persistence of horizontal temperature gradients is diabatically forced in the same way.

The role of diabatic effects can be contrasted with a more dynamical perspective such as Pinto et al. (2014), but here it is also not clear to what extent the observed large-scale Rossby wave breaking drives cyclone clustering or mainly diagnoses the concomitant high eddy activity.

The simulated storm tracks have some hard to mitigate biases, both in forecasting context (Rodwell et al., 2013) as well as climate context (Zappa et al., 2013). We need to better understand the dynamics of baroclinicity itself to make progress on these issues. We propose to reformulate baroclinicity in the N. Atlantic to a simple but accurate description in terms of mean dry entropy at the northern edge of the storm track genesis region, demonstrating that this determines synoptic time-scale variability in the storm track, rather than detailed processes within the storm track itself.

2 Eady growth rate and thermal wind balance

In this study we use two-hourly reanalysis data for December, January, and February from ERA5 (Hersbach, 2020), starting from December 1991 and ending in February of 2021. Our focus is on the lower free troposphere, so we consider a range of pressure levels from 800 hPa to 750 hPa. To study baroclinicity in the N. Atlantic storm track we use a 0.25° horizontal grid covering the region $15-80$ N and -$105-15$ E as illustrated in Fig. 1.

The Eady growth rate is usually defined as

$$\sigma_u = 0.31 \frac{|f|}{N} \frac{\partial u}{\partial z} \tag{1}$$

where f is the Coriolis parameter, N is the Brunt Väisälä frequency, and $\partial u/\partial z$ is the vertical shear of the zonal wind. For the southern hemisphere a minus sign would be introduced in this equation. Here, the subscript u refers to the measure's dependence on vertical wind shear.

Using the thermal wind relation, σ_u can be rearranged in terms of a gradient in dry specific entropy, $\partial s/\partial y$. Because the thermal wind relation is not often considered in height coordinates (usually pressure or log-pressure coordinates are used) we

https://doi.org/10.5194/egusphere-2026-3043
Preprint. Discussion started: 11 June 2026

write this out explicitly here. We begin with geostrophic balance in pressure coordinates, considering only the zonal wind u and using Cartesian coordinates

$$fu = -\left(\frac{\partial \Phi}{\partial y}\right)_p, \tag{2}$$

where Φ is geopotential (Hoskins and James, 2014). Taking the vertical (pressure) derivative then leads to thermal wind balance in pressure coordinates.

$$f\frac{\partial u}{\partial p} = \frac{R}{p}\left(\frac{\partial T}{\partial y}\right)_p. \tag{3}$$

The subscript p indicates that the meridional derivative is taken at constant pressure. We used hydrostatic balance in pressure coordinates $(\partial\Phi/\partial p) = 1/\rho = RT/p$ and the ideal gas law as relevant to the Eady model.

Hydrostatic balance also allows us to locally map pressure derivatives to height derivatives according to

$$\mathrm{d}\ln p = -\frac{g}{RT}\mathrm{d}z. \tag{4}$$

From this we can construct the relevant form of thermal wind balance

$$f\frac{\partial u}{\partial z} = -\frac{g}{T}\left(\frac{\partial T}{\partial y}\right)_p = -\frac{g}{c_p}\left(\frac{\partial s}{\partial y}\right)_p, \tag{5}$$

where we introduce the dry specific entropy s for an ideal gas, which depends on temperature and pressure as

$$\mathrm{d}s = c_p\frac{\mathrm{d}T}{T} - R\frac{\mathrm{d}p}{p}. \tag{6}$$

Using this form of the thermal wind relation we can express baroclinicity in terms of the meridional gradient of dry entropy,

$$\sigma_s = -0.31\,\frac{g}{c_p N}\left(\frac{\partial s}{\partial y}\right)_p. \tag{7}$$

Here, the subscript s refers to the measure's dependence on dry entropy. The sign of this equation is relevant for the northern hemisphere; for the southern hemisphere the minus sign is removed. Note again that the meridional derivative of entropy is taken at constant pressure, allowing computation of the Eady growth rate using data at a single pressure level and without using vertical finite differences.

The rewritten version in Eq. 7 has the same level of validity as the more commonly encountered form from Eq. 1. The quasi-geostrophic model that defines the Eady growth rate as the relevant growth rate for baroclinic eddies is both geostrophic and hydrostatic, so in that context the two forms are equivalent.

To compare the two forms of Eady growth rate, σ_u and σ_s, from real world data, Fig. 1 shows the difference of 30 winter (DJF) climatologies over the N. Atlantic. Within the storm track σ_s is found to be greater than σ_u, with the opposite being true over N. Africa. These match approximately the positions of the climatological low and high pressure regions associated with the N. Atlantic storm track. Gradient wind balance gives a plausible explanation for these differences, as the wind about

https://doi.org/10.5194/egusphere-2026-3043
Preprint. Discussion started: 11 June 2026

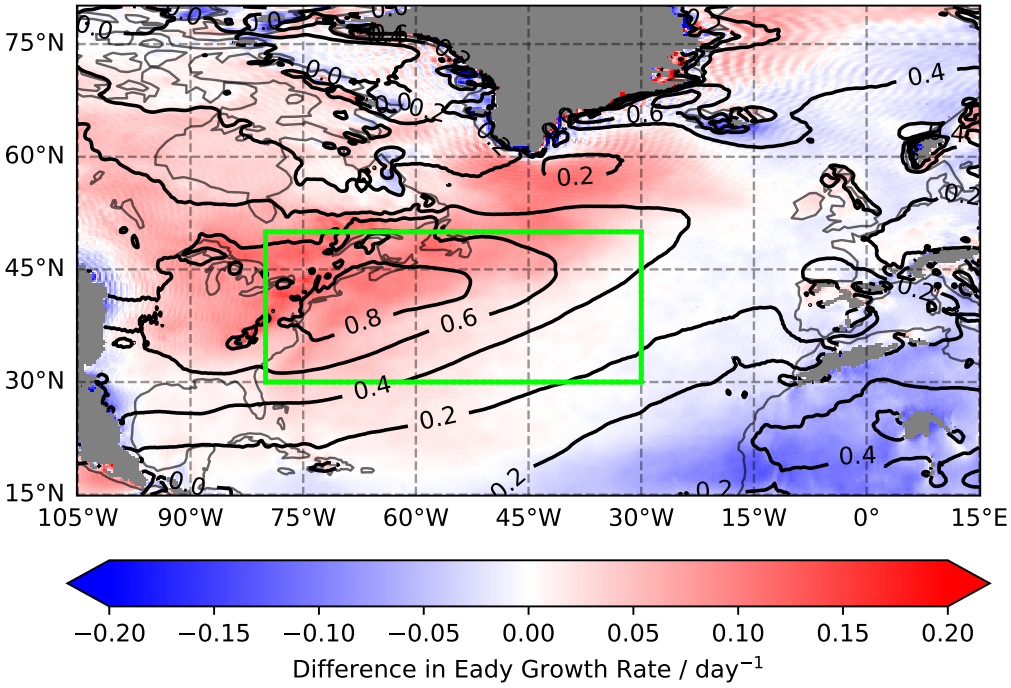

Figure 1. Comparison of forms of the Eady growth rate, σ_u (Eq. 1) and σ_s (Eq. 7). Contours show a 30 winter (1991–2021; DJF) climatological mean of σ_s in units of day^{-1} at 775 hPa. Colours show the climatological mean difference $\sigma_s - \sigma_u$ (i.e. σ_s is larger where values are positive). Stability N is calculated using Eq. 8 at 775 hPa at each grid point, with the derivative computed as a finite difference between 750 and 800 hPa. Surface heights above 1 km are masked in grey. The region commonly used in our analysis, 15 – 80 N and -105 – 15 E, is outlined in green.

a low pressure system can be *subgeostrophic*, meaning an outward centrifugal force allows consistently slower speeds than the geostrophic wind, with faster *supergeostrophic* winds about a high pressure system. This suggests that around a climatological low σ_u is smaller than σ_s and vice versa around a climatological high. Assuming thermal wind balance, σ_u and σ_s are equal, so the differences between them are the result of ageostrophic effects and as such would not contribute to the quantification of baroclinic growth in a quasi-geostrophic context.

The Eady growth rate from Eq. 1, σ_u, features a diurnal cycle which does not appear in σ_s, a consequence of the top of the boundary layer increasing and decreasing in height from day to night (Marcheggiani and Ambaum, 2020). During the day, the top of the boundary layer raises and frictional effects result in a slowing of the wind, meaning wind shear in the lower troposphere increases. This effect is more pronounced over land than ocean and contributes small, high frequency numerical changes that don't represent meaningful differences in the growth rate of baroclinic instabilities. Since our calculation of baroclinicity with Eq. 7 is mainly dependent on a single pressure level, the pressure at which we calculate $\partial s/\partial y$, it does not share this issue. To better compare the two fields, a 24–hour running mean filter is hereafter applied to σ_u.

https://doi.org/10.5194/egusphere-2026-3043
Preprint. Discussion started: 11 June 2026

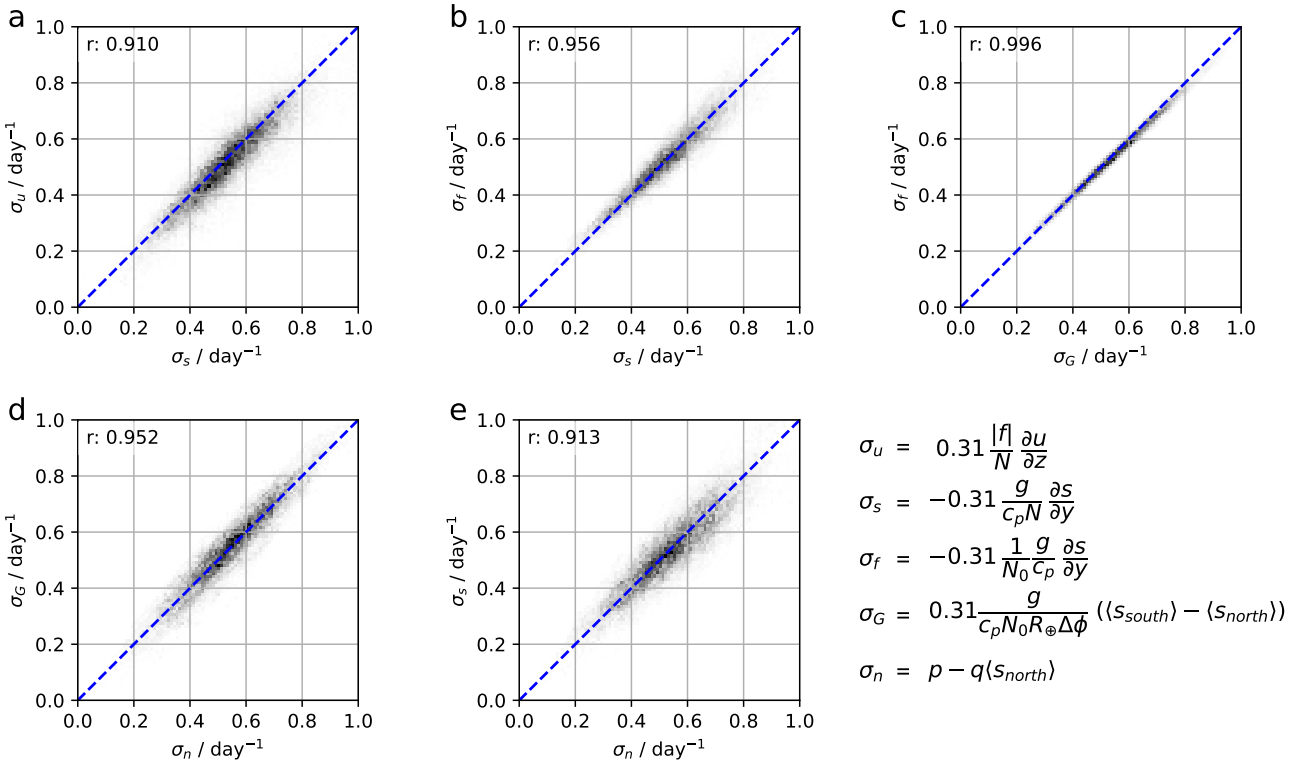

Figure 2. Comparisons of calculation methods of two hourly area average baroclinicity in the storm track region ($30-50$N, $30-80$W) across the 30 winters (DJF) from 1991 to 2021. In all plots the 1–1 line is shown in dashed blue. Each plot shows the Eady growth rate calculated with: **(a)** a zonal wind shear dependence (σ_u, Eq. 1), compared with a meridional entropy gradient dependence (σ_s, Eq. 7); **(b)** a meridional entropy gradient dependence (σ_s, Eq. 7), with stability N calculated as Eq. 8, compared with the same equation but where stability is a fixed parameter (σ_f, Eq. 9); **(c)** a meridional entropy gradient dependence with fixed stability (σ_f, Eq. 9), compared with σ_G (Eq. 12) where Green's theorem is applied; **(d)** the Green's theorem version (σ_G, Eq. 12) compared with a linear regression where only $\langle s_{north} \rangle$ varies (σ_n, Eq. 13); **(e)** a meridional entropy gradient dependence (σ_s, Eq. 7), with stability N as a horizontally varying field compared with a linear regression where only $\langle s_{north} \rangle$ varies (σ_n, Eq. 13). The table in the bottom right shows the expressions used.

Figure 2a compares two-hourly area mean baroclinicity in the N. Atlantic storm track region over 30 winters calculated as σ_u and σ_s to demonstrate that the variability of these expressions are comparable. The mean and variance for σ_u are $0.53\,\text{day}^{-1}$ and $0.022\,\text{day}^{-1}$ respectively, the mean and variance for σ_s are $0.54\,\text{day}^{-1}$ and $0.023\,\text{day}^{-1}$, and the Pearson correlation coefficient between them is 0.91. Mean, variance, and correlations for each formulation of σ are found in Table 1 and Table 2.

While there are numerical differences between σ_u and σ_s, both are valid expressions of the Eady growth rate since their applicability is only defined in the quasi-geostrophic framework, where the two expressions are equivalent. The similarity in variability of these measures of baroclinicity further validates using σ_s to express the Eady growth rate in the real atmosphere.

https://doi.org/10.5194/egusphere-2026-3043
Preprint. Discussion started: 11 June 2026

The Brunt Väisälä frequency is

$$N = \left(\frac{g}{\theta} \frac{\partial \theta}{\partial z} \right)^{1/2}, \tag{8}$$

where g is acceleration due to gravity and θ is potential temperature. This is commonly computed locally, however, since the Eady growth rate arises from quasi-geostrophic dynamics where N is a fixed parameter, constant in time and across surfaces of constant pressure, there is a theoretical justification to treat N as a given constant on a pressure level. To justify this approach in practice, we now show that the role of local variability in N, or more specifically $1/N$, in the Eady growth rate is small compared to contributions from the horizontal temperature gradients.

To treat $1/N$ as a parameter we need first to find its optimum value. This is not the same as calculating mean N for our region and period, rather we use a least squares fit between σ_s, where σ_s is calculated with Eq. 7, and $N \cdot \sigma_s$, removing stability from the denominator of Eq. 7, in order to find the best fit value, $1/N_0$. This method gives the optimum value of N as $N_0 = 0.01484\,\mathrm{s}^{-1}$. Considering stability to be fixed, we then express the Eady growth rate as

$$\sigma_f = -0.31 \frac{1}{N_0} \frac{g}{c_p} \left(\frac{\partial s}{\partial y} \right)_p. \tag{9}$$

Figure 2b compares σ_s, where N computed instantaneously and locally, with σ_f, where we use the optimum value of stability. Statistical comparisons are repeated in Table 2 and Table 1, demonstrating that allowing stability to vary does not make a meaningful difference to area mean baroclinicity in the storm track. As such we will treat it as a fixed parameter henceforth.

3 An entropy framework for area mean baroclinicity

Baroclinic instabilities are large scale wave instabilities, growing on a baroclinically unstable background. Smaller scale details in the temperature gradients will modify local values of the Eady growth rate, but we hypothesise they do not play a substantial role in the growth rate of baroclinic waves; these will be sensitive to the larger scale temperature gradients only. Therefore, we are mainly interested in the area mean Eady growth rate, where the area is chosen to contain the strong baroclinic region of the storm track.

The area mean baroclinicity for a geographically confined region A is

$$\overline{\sigma_f} = \frac{1}{A} \iint_A \sigma \, \mathrm{d}A = -0.31 \frac{g}{c_p N_0 A} \iint_A \frac{\partial s}{\partial y} \, \mathrm{d}A. \tag{10}$$

Given the integrand is a meridional derivative, we next explore the extent to which we can approximate the integration by omitting the cosine latitude dependence. We can then interpret $\mathrm{d}A$ as the Cartesian measure of area (that is, $\mathrm{d}A = \mathrm{d}x\mathrm{d}y$) and use Green's integral theorem (Marsden and Tromba, 1996), to write

$$\overline{\sigma_f} = 0.31 \frac{g}{c_p N_0 A} \oint_{\partial A} s \, \mathrm{d}x. \tag{11}$$

where ∂A is the positively oriented boundary of area A, and x is the zonal coordinate. For the S. Hemisphere a minus-sign is introduced to this expression.

https://doi.org/10.5194/egusphere-2026-3043
Preprint. Discussion started: 11 June 2026

Performing this contour integral over the latitude–longitude box, we find

$$\sigma_G = 0.31 \frac{g}{c_p N R_\oplus \Delta\phi} \left(\langle s_{\text{south}} \rangle - \langle s_{\text{north}} \rangle \right), \tag{12}$$

where $R_\oplus$ is Earth's radius in metres, $\Delta\phi$ is the difference of the latitudinal edges of the integrated region in radians, and s_{south} and s_{north} represent the specific entropy along the meridional borders of the region closest to the equator and pole respectively, with angled brackets denoting the mean across the latitude line.

Using Eq. 12, mean baroclinicity can be calculated for a region with just a rescaling of the difference in specific entropy along its meridional borders. This means that baroclinicity in a region can be enhanced with an increase or decrease in entropy on the equatorward or poleward side of a baroclinic zone respectively; any internal variations in baroclinicity that do not alter these mean boundary values do not contribute to variations in the mean baroclinicity.

Figure 2c compares σ_s with σ_G, the difference being that σ_s uses an area mean and σ_G uses a grid mean where all model cells are considered as having equal area. It is clear visually that applying the Green's theorem makes little difference to the spread of the data. In other words, considering a Cartesian mean rather than the area mean does not change the measure of baroclinicity in any relevant way. The mean, variance, and correlation of these measures can be found in Table 1 and Table 2.

Equal changes in entropy along either the north or south border of the storm track have an identical effect on σ_G, though entropy along the north border varies more than to the south, as is shown in Fig. 3. We quantify this difference with their variances over the 30 winter period, being $44\,\text{J}\,\text{kg}^{-1}\,\text{K}^{-1}$ for $\langle s_{\text{south}} \rangle$, smaller than the variance of $\langle s_{\text{north}} \rangle$ which is $362\,\text{J}\,\text{kg}^{-1}\,\text{K}^{-1}$. This indicates that the variance in the area mean baroclinicity in the N. Atlantic storm track is mainly determined by processes on its north border.

Figure 3 also shows that there is not a strong seasonal cycle in $\langle s_{\text{south}} \rangle$ relative to variability in $\langle s_{\text{north}} \rangle$, rather $\langle s_{\text{south}} \rangle$ mainly contributes noise to σ_G. We can therefore treat $\langle s_{\text{south}} \rangle$ as a constant during winter while preserving much of the variability in σ_G. This allows us to express the Eady growth rate, through a linear regression, as dependent on $\langle s_{\text{north}} \rangle$ as its only variable. Performing this linear regression between $\langle s_{\text{north}} \rangle$ and σ_G gives the expression

$$\sigma_n = p - q \langle s_{\text{north}} \rangle, \quad p = 0.797\,\text{day}^{-1}, \quad q = 1.0496 \frac{0.31 g}{c_p N_0 R_\oplus \Delta\phi}, \tag{13}$$

where p is a fitting constant mainly determined by $\langle s_{\text{south}} \rangle$ and q is a scaling derived from the linear regression.

From this linear regression it is clear that entropy along the north boundary of our storm track region is the main factor determining variations in baroclinicity in the region, as the coefficient ahead of the constants in the q term is near 1. The fact that the coefficient is not exactly 1 accounts for the covariability between $\langle s_{\text{north}} \rangle$ and $\langle s_{\text{south}} \rangle$; that this coefficient is slightly above 1 indicates weak negative covariability.

We can compare Eq. 13 with an equivalent where we replace $\langle s_{\text{north}} \rangle$ with $\langle s_{\text{south}} \rangle$ to give σ_{south}, repeating the statistical comparison with Eq. 12 to find that the correlation coefficient decreases from 0.95 to 0.38. Additionally, the variance for σ_{south} decreases to $0.0049\,\text{day}^{-1}$, demonstrating its poor similarity to σ_G which has a variance of $0.025\,\text{day}^{-1}$. Entropy at the two borders is weakly anti-correlated, with a correlation coefficient between $\langle s_{\text{north}} \rangle$ and $\langle s_{\text{south}} \rangle$ of -0.15, making it unsurprising that $\langle s_{\text{south}} \rangle$ provides a worse estimate of baroclinicity. This further demonstrates that variability in area mean baroclinicity is determined by processes altering temperature to the north, rather than processes internal to or south of the storm track.

https://doi.org/10.5194/egusphere-2026-3043
Preprint. Discussion started: 11 June 2026

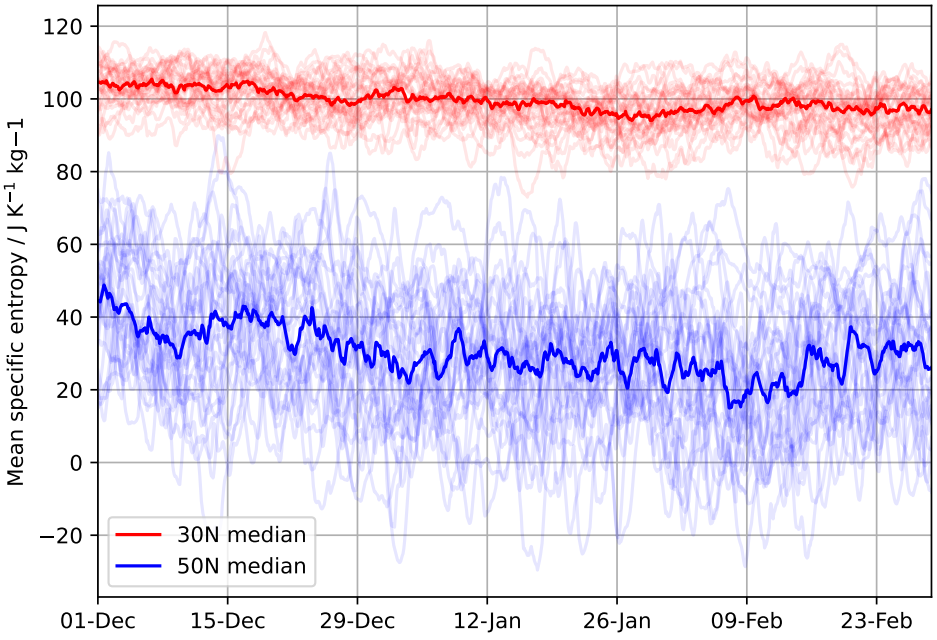

Figure 3. 775 hPa mean specific entropy along the $30-80$ W latitude line at 30 N (red) and 50 N (blue). Faint lines show individual years in our 30 winter climatology, while bold lines show the median across the climatology. The climatological mean shows a similar patten to the median, except with less variance.

Comparing σ_n with σ_G in Fig. 2d demonstrates that by removing any dependence on $\langle s_{\text{south}} \rangle$ the Eady growth rate is not significantly affected numerically. By design of the linear regression, the two expressions share a mean value, $0.55\,\text{day}^{-1}$, but the variance in σ_n is slightly lower, decreasing from $0.025\,\text{day}^{-1}$ to $0.023\,\text{day}^{-1}$, showing the weaker variability in entropy to the south and suggesting $\langle s_{\text{south}} \rangle$ was introducing noise rather than a coherent signal contributing to changes in baroclinicity.

As shown, synoptic-timescale variations in area mean baroclinicity are mainly determined by entropy-changing processes on the poleward side of the storm track. Such processes include cold-air outbreaks originating from North-America and the Labrador Sea.

In this manipulation of the Eady growth rate, we began with an agreed upon expression with variables $\partial u/\partial z$ and $1/N$ (Eq. 1), applied thermal wind balance to replace the zonal wind shear term with $(\partial s/\partial y)_p$ (Eq. 7), treated the variable $1/N$ as a parameter so $(\partial s/\partial y)_p$ is the only variable (Eq. 9), applied the Green's integration theorem to reduce area mean growth rate to a scaling of the difference in mean entropy between the north and south borders (Eq. 12), and performed a linear regression to express the Eady growth rate with $\langle s_{\text{north}} \rangle$ as its only variable (Eq. 13).

https://doi.org/10.5194/egusphere-2026-3043
Preprint. Discussion started: 11 June 2026

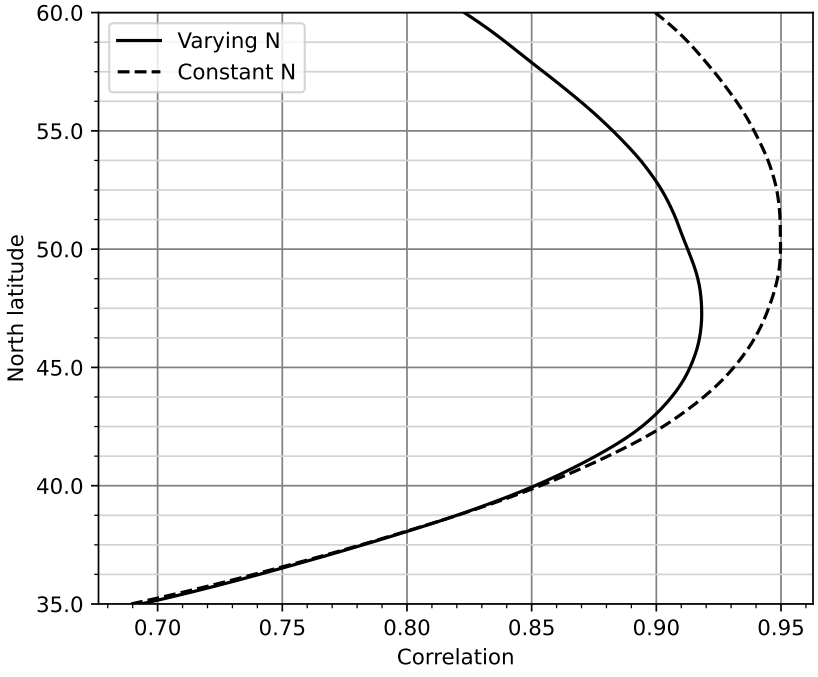

Figure 4. Correlation between 30 winter (DJF) area-mean baroclinicity σ_s in the region 30-(north)N, 30-80W (where north is given on the y-axis), and $\langle s_{\text{north}} \rangle$ at 775hPa. For the bold line stability N is calculated with Eq. 8 between 750 and 800hPa, and for the dashed line an optimum value is used. The optimum value of stability is calculated with a least-squares fit method outlined previously.

The difference between σ_s and σ_u is entirely physical, because it measures the lack of geostrophic balance in the storm track. In the quasi-geostrophic context, which underpins the physical relevance of the Eady growth rate, the two expressions are equivalent, meaning that we can use the expression σ_s as our benchmark to compare our final result with. Figure 2e compares σ_n with σ_s, demonstrating that these steps, which all introduce moderate numerical differences due to the simplifying choices we made, do not dramatically affect the values of the inferred growth rate. The total change introduced in going from σ_s to σ_n is in fact less than the difference between σ_u and σ_s which are, as discussed, both equally valid forms of the Eady growth rate.

Throughout this work we consider the upstream region of the N. Atlantic storm track well contained in the area $30-50$N, $30-80$W, focussing largely on the north edge of this area. This box contains the most active region of the storm track, particularly in terms of the genesis of cyclones. We now determine the latitude range for which the linear regression used in Eq. 13 obtains good results.

Figure 4 shows the changing correlation coefficient between σ_s and σ_n as the north edge of our chosen region is adjusted. The edges of the box are otherwise fixed at 30N, 30W, and 80W. For each new latitude for the north edge of the region, the optimum stability N_0 is recalculated along with new parameters in Eq. 13 for the linear regression for σ_n. With stability treated

https://doi.org/10.5194/egusphere-2026-3043
Preprint. Discussion started: 11 June 2026

Table 1. Mean and variance for different forms of the Eady growth rate.

	Mean / day^{-1}	Variance / day^{-1}
σ_u	0.53	0.022
σ_s	0.54	0.023
σ_f	0.54	0.023
σ_G	0.55	0.025
σ_n	0.55	0.023
σ_{south}	0.55	0.0049

Table 2. Correlations for different forms of the Eady growth rate.

	σ_u	σ_s	σ_f	σ_G	σ_n	σ_{south}
σ_u	1.00					
σ_s	0.91	1.00				
σ_f	0.91	0.96	1.00			
σ_G	0.91	0.94	0.996	1.00		
σ_n	0.86	0.91	0.95	0.95	1.00	
σ_{south}	0.41	0.38	0.44	0.38	0.15	1.00

as a varying field the correlation peaks with a value of 0.92 where the northern edge is at 47.25 N, and where an optimum value of stability, N_0, is computed for each adjustment of the north latitude the peak in correlation is at 50 N with a value of 0.95.

It is clear that the relationship described between area mean baroclinicity in the storm track and $\langle s_{\text{north}} \rangle$ is not uniquely found at 50 N, as there is a wide band of latitudes where the correlation remains high, though 50 N exhibits the strongest correlation, which justifies its use.

4 Conclusions

We have demonstrated that the Eady growth rate can be rearranged through thermal wind balance to be dependent on a meridional entropy gradient, eliminating much of the high–frequency variation found when it is calculated using zonal wind shear. These oscillations associated with the diurnal cycle do not contribute to the development of baroclinic instabilities, so reducing them provides a more coherent estimation of baroclinicity without requirement of time filtering. This form of baroclinicity, σ_s (Eq. 7), is equally valid as its more common expression, σ_u (Eq. 1), as each are equivalent within the context of the validity of the Eady model used to diagnose growth rates.

https://doi.org/10.5194/egusphere-2026-3043
Preprint. Discussion started: 11 June 2026

The lack of geostrophic balance introduces a numerical difference between the two measures. Their common variance is 83%, suggesting that the quantitative determination of physically relevant area mean baroclinicity has a minimum uncertainty variance of around 17%; there is no real benefit in improving measures of baroclinicity beyond this uncertainty, because the two physically equivalent measures already have this level of discrepancy.

We have shown that mean baroclinicity in the N. Atlantic storm track can be accurately approximated by a linear regression of mean dry entropy to the north of the storm track, with 83% of the variability in area mean baroclinicity in our chosen region being captured by $\langle s_{\text{north}} \rangle$. Our data has a two-hour resolution and therefore contains variability of all frequencies up to the Nyquist frequency of $6\,\text{day}^{-1}$. Any time filtering would further enhance this correspondence.

Because the variability of the area mean baroclinicity is well captured by entropy at the north border of the storm track, any processes that modify the temperature field inside the storm track region, such as latent heat release and other frontal effects, only have a bearing on area mean baroclinicity insofar as these processes also modify the mean entropy at the north border. It also means that processes outside the storm track region can modify the area mean baroclinicity as long as these these processes also modify the mean entropy at the north border of the storm track.

Our results also indicate that a dynamical budget for area mean baroclinicity is actually quite simple: it just requires a temperature tendency equation averaged over the northern border of the storm track. We are currently investigating what the implications of this simplification is for understanding the dynamics of the N. Atlantic storm track.

Author contributions. R.Biddiscombe and M.H.P. Ambaum conceived of the work. R. Biddiscombe performed the data analysis, visualisations, and wrote the work. M.H.P. Ambaum and B. Harvey gave scientific advice and suggestions for the written work.

Competing interests. The authors have no competing interests.

Acknowledgements. R. Biddiscombe acknowledges financial support from the NERC SCENARIO DTP.

https://doi.org/10.5194/egusphere-2026-3043
Preprint. Discussion started: 11 June 2026

References

Ambaum, M. H. P. and Novak, L.: A nonlinear oscillator describing storm track variability, Quarterly Journal of the Royal Meteorological Society, 140, 2680–2684, 2014.

Binder, H., Boettcher, M., Joos, H., and Wernli, H.: The Role of Warm Conveyor Belts for the Intensification of Extratropical Cyclones in Northern Hemisphere Winter, Journal of the Atmospheric Sciences, 73, 3997 – 4020, https://doi.org/10.1175/JAS-D-15-0302.1, 2016.

Blackmon, M. L., Wallace, J. M., Lau, N.-C., and Mullen, S. L.: An Observational Study of the Northern Hemisphere Wintertime Circulation, Journal of Atmospheric Sciences, 34, 1040 – 1053, https://doi.org/10.1175/1520-0469(1977)034<1040:AOSOTN>2.0.CO;2, 1977.

Eady, E. T.: Long Waves and Cyclone Waves, Tellus, 1, 33–52, https://doi.org/https://doi.org/10.1111/j.2153-3490.1949.tb01265.x, 1949.

Federer, M., Papritz, L., Sprenger, M., Grams, C. M., and Wenta, M.: On the Local Available Potential Energy Perspective of Baroclinic Wave Development, Journal of the Atmospheric Sciences, 81, 871 – 886, https://doi.org/10.1175/JAS-D-23-0138.1, 2024.

Hersbach, H. e. a.: The ERA5 global reanalysis, Quarterly Journal of the Royal Meteorological Society, 146, 1999–2049, https://doi.org/https://doi.org/10.1002/qj.3803, 2020.

Hoskins, B. J. and James, I. N.: Fluid Dynamics of the Midlatitude Atmosphere, chap. 5, John Wiley Sons, Ltd, ISBN 9781118526002, 2014.

Hoskins, B. J. and Valdes, P. J.: On the Existence of Storm-Tracks, Journal of Atmospheric Sciences, 47, 1854 – 1864, https://doi.org/https://doi.org/10.1175/1520-0469(1990)047<1854:OTEOST>2.0.CO;2, 1990.

Lindzen, R. S. and Farrell, B.: A Simple Approximate Result for the Maximum Growth Rate of Baroclinic Instabilities, Journal of Atmospheric Sciences, 37, 1648 – 1654, https://doi.org/10.1175/1520-0469(1980)037<1648:ASARFT>2.0.CO;2, 1980.

Marcheggiani, A. and Ambaum, M. H. P.: The role of heat-flux–temperature covariance in the evolution of weather systems, Weather and Climate Dynamics, 1, 701–713, https://doi.org/10.5194/wcd-1-701-2020, 2020.

Marsden, J. E. and Tromba, A. J.: Vector Calculus, W. H. Freeman and Company, 4 edn., 1996.

Papritz, L. and Spengler, T.: Analysis of the slope of isentropic surfaces and its tendencies over the North Atlantic, Quarterly Journal of the Royal Meteorological Society, 141, 3226–3238, 2015.

Pinto, J. G., Gómara, I., Masato, G., Dacre, H. F., Woollings, T., and Caballero, R.: Large-scale dynamics associated with clustering of extratropical cyclones affecting Western Europe, Journal of Geophysical Research: Atmospheres, 119, 13,704–13,719, https://doi.org/https://doi.org/10.1002/2014JD022305, 2014.

Rodwell, M. J., Magnusson, L., Bauer, P., Bechtold, P., Bonavita, M., Cardinali, C., Diamantakis, M., Earnshaw, P., Garcia-Mendez, A., Isaksen, L., Källén, E., Klocke, D., Lopez, P., McNally, T., Persson, A., Prates, F., and Wedi, N.: Characteristics of Occasional Poor Medium-Range Weather Forecasts for Europe, Bulletin of the American Meteorological Society, 94, 1393 – 1405, https://doi.org/10.1175/BAMS-D-12-00099.1, 2013.

Simmons, A. J. and Hoskins, B. J.: The Downstream and Upstream Development of Unstable Baroclinic Waves, Journal of Atmospheric Sciences, 36, 1239 – 1254, https://doi.org/10.1175/1520-0469(1979)036<1239:TDAUDO>2.0.CO;2, 1979.

Weijenborg, C. and Spengler, T.: Diabatic Heating as a Pathway for Cyclone Clustering Encompassing the Extreme Storm Dagmar, Geophysical Research Letters, 47, 2020.

Zappa, G., Shaffrey, L. C., Hodges, K. I., Sansom, P. G., and Stephenson, D. B.: A Multimodel Assessment of Future Projections of North Atlantic and European Extratropical Cyclones in the CMIP5 Climate Models, Journal of Climate, 26, 5846 – 5862, https://doi.org/10.1175/JCLI-D-12-00573.1, 2013.